Online Determination of Total Radiated Power by Bolometric Cameras with Statistical Methods

M. Maraschek, J.C. Fuchs, F. Mast, V. Mertens, H. Zohm

IPP 1/297 April 1996

MAX-PLANCK-INSTITUT FÜR PLASMAPHYSIK

85748 GARCHING BEI MÜNCHEN

MAX-PLANCK-INSTITUT FÜR PLASMAPHYSIK

GARCHING BEI MÜNCHEN

Online Determination of Total Radiated Power by Bolometric Cameras with Statistical Methods

M. Maraschek, J.C. Fuchs, F. Mast, V. Mertens, H. Zohm

IPP 1/297 April 1996

Die nachstehende Arbeit wurde im Rahmen des Vertrages zwischen dem Max-Planck-Institut für Plasmaphysik und der Europäischen Atomgemeinschaft über die Zusammenarbeit auf dem Gebiete der Plasmaphysik durchgeführt.

March 29, 1996

Abstract

In order to control the puffing of impurities (neon,argon) and deuterium gas in the main plasma chamber for experiments with a radiative boundary, a fast online determination of the total radiated power from the plasma for a feedback control is required. The total radiated power is normally calculated by a deconvolution of measurements of a horizontal bolometer camera with 40 lines of sight. This time consuming algorithm, which works under the assumption of constant emissivity on closed flux surfaces, can not be used online during the experiment to reach the so called CDH-mode [1, 2].

By means of a singular value decomposition a subset of 10 and 18 channels of the horizontal bolometric camera system is chosen for online reconstruction of the radiated power. A new nontrivial selection scheme was established for this purpose. With this subset a regression analysis against the offline calculated power was done. The regression coefficients are then used for a weighted sum over the selected subset of lines of sight to predict the total radiated power online during the discharge.

1 Experimental Setup

The total radiated power from a Tokamak plasma is normally calculated from the measurements of a bolometric camera system. In this section the bolometric system on ASDEX Upgrade and the tools for calculating the total radiated power from the plasma online during the discharge are described.

1.1 Bolometric Camera System on ASDEX Upgrade

On ASDEX Upgrade a bolometric camera system with 88 channels exists. The majority of them is arranged in one horizontal camera with 40 lines of sight and one vertical camera with 24 lines of sight. The locations and the lines of sight in a poloidal plane

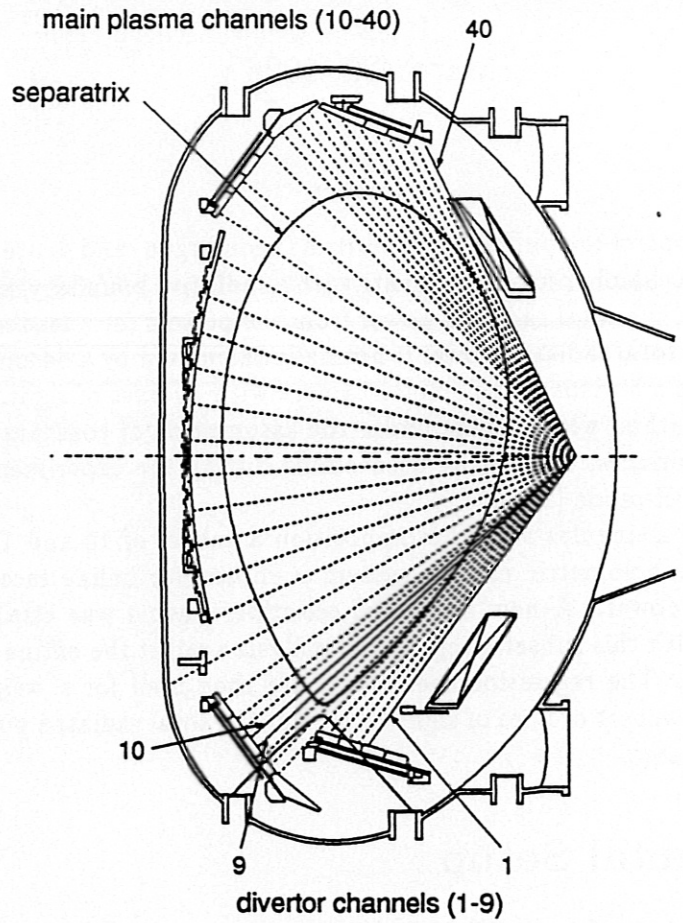

Figure 1: location and lines of sight of the horizontal bolometric camera system

are shown in figure 1. In this cross section also the separatrix of a typical single null plasma with the X-point at the lower divertor is shown.

From the horizontal camera the total radiated power from the main plasma is calculated offline by a weighted summation of the intensities from the selected channels. This is done under the assumption of constant emissivity on closed flux surfaces. For this inversion only the lines of sight above the X-point of the plasma are used and the channels below the X-point are neglected (no closed flux surfaces anymore) [3].

1.2 Weighted Summation over a Subset of Lines of Sight

For a fast online determination of the total radiated power a hardware tool exists, which can build the weighted sum over 10 and newly 18 channels. This number of channels is the maximum amount of lines of sight, which can be used for the online

prediction of the radiated power by a weighted summation

$$P_{rad} = \sum_{i=1}^{10/18} c_i \cdot (\int \xi(\vec{r}) \cdot dl)_i, \tag{1}$$

where $\xi(\vec{r})$ represents the local emissivity from the plasma, and $(\int \xi(\vec{r}) \cdot dl)_i$ the line integral of the intensity from each line of sight from the bolometer camera. The physical unit of the bolometer camera is $\frac{W}{m^2}$, the unit of the radiated power is W. It is obvious that the requested coefficients have then the unit m^2.

The selection of the channels and the determination of the corresponding coefficients is done in 4 steps:

1. Choose existing discharges for the analysis and for a test before implementing the algorithm (step 1)
2. Determine the relevant channels of the bolometer system (step 2)
3. Determine the coefficients c_i to get the total radiated power form the selected channels (step 3)
4. Test the results by predicting the total radiated power for existing discharges with the selected channels and the calculated coefficients, where the offline signal is already available (Step 4)

2 Statistical Methods

In this section a brief description of the used statistical methods is given. Two methods, namely a Singular Value Decomposition for discarding variables and a linear regression analysis for the determination of the weights for the online determination of the total radiated power were used.

2.1 Singular Value Decomposition (SVD)

At each time t_i during a discharge one gets a p-dimensional vector $\vec{x}_i = \vec{x}(t_i)$, or $x_{ij} = x_j(t_i)$ of measurements. In our case one deals with $p = 40$ measurements from the horizontal bolometric camera. Considering all measurement-vectors at the N times ($N \geq p$) during the discharge one can order the data in a $N \times p$ matrix of measurements

$$\mathbf{X} = \begin{pmatrix} x_{11} & x_{12} & \cdots & x_{1p} \\ x_{21} & x_{22} & \cdots & x_{2p} \\ \vdots & \vdots & \ddots & \vdots \\ x_{N1} & x_{N2} & \cdots & x_{Np} \end{pmatrix}. \tag{2}$$

It is now possible to represent the data matrix in a new orthonormal coordinate system

$$\mathbf{X} = \sum_{k=1}^{p} \sqrt{\lambda_k}\vec{b}_k \cdot \vec{a}_k^T, \tag{3}$$

which can be written in compact matrix notation

$$\mathbf{X} = \mathbf{BDA}^T. \tag{4}$$

In this system the projection of the data points on the new axes with the base vectors $\vec{b}_k$ and $\vec{a}_k$ are maximized. The terms in the sum (3) are ordered in descending order of magnitude of λ_k.

One can prove [4, 5] that the desired base vectors are the normalized eigenvectors of the real symmetric matrices $\mathbf{S} = \mathbf{X}^T\mathbf{X}$ and $\mathbf{T} = \mathbf{X}\mathbf{X}^T$ respectively.

$$\mathbf{S}\vec{a}_k = \lambda_k\vec{a}_k, \qquad \mathbf{T}\vec{b}_k = \lambda'_k\vec{b}_k. \tag{5}$$

These matrices are called the "*sums of squares and cross-products matrix*". The eigenvectors from $\mathbf{S}$ and $\mathbf{T}$ are called spatial and temporal eigenvectors respectively. The corresponding eigenvalues λ_k measure the maximal mean elongation of the data points with respect to the corresponding eigenvector (base vector). In this system $\mathbf{S}$ and $\mathbf{T}$ are diagonal matrices with the eigenvalues λ_k as diagonal elements. It can be shown that the quantities in the two spaces of $\mathbf{S}$ and $\mathbf{T}$ are connected by the following relations

$$\lambda'_k = \lambda_k, \qquad \vec{b}_k = \frac{1}{\sqrt{\lambda_k}}\mathbf{X}\vec{a}_k, \quad \vec{a}_k = \frac{1}{\sqrt{\lambda_k}}\mathbf{X}^T\vec{b}_k. \tag{6}$$

Instead of using the sums of squares and cross-products matrices one can also use the covariance or correlation matrices with respect to time

$$s_{ij} = \frac{1}{N-1}\sum_{k=1}^{N}(x_{ki} - \langle x_i\rangle)(x_{kj} - \langle x_j\rangle), \tag{7}$$

$$\rho_{ij} = \frac{1}{N-1}\sum_{k=1}^{N}\frac{(x_{ki} - \langle x_i\rangle)}{\sqrt{s_{ii}}}\frac{(x_{kj} - \langle x_j\rangle)}{\sqrt{s_{jj}}}. \tag{8}$$

The eigenvalues now represent the variance or the correlation coefficient of the data points in the direction of the corresponding eigenvector respectively. Normalized to the total variance of the covariance matrix, it measures the degree of information α of the direction for the complete data set

$$\alpha_i = \frac{\lambda_i}{\sum_{j=1}^{p}\lambda_j} = \frac{\lambda_i}{\mathrm{Trace}(s_{ij})}. \tag{9}$$

In the context of this work only the sums of squares and cross-products matrices was used.

2.2 Discarding of Variables (Channels) by SVD, Step 2

In order to determine the relevant channels a singular value decomposition was used. This SVD is applied to a set of existing discharges which have to be selected in the first step (see chapter 3.1). There were three different methods tested how the relevant channels can be chosen.

The first approach for selecting variables or better channels is to analyze the first spatial eigenvectors with the greatest eigenvalues. These eigenvectors represent the dominant information, e.g. the emission profile from the camera. For a certain amount of dominant, e.g high eigenvalues one selects those channels which have the highest amplitude in the corresponding spatial eigenvectors. All the remaining channels with lower amplitude are neglected.

A completely different approach was suggested by [6] for discarding unimportant channels instead of selecting important ones. One considers the eigenvectors with the smallest eigenvalues and discards, starting with the lowest eigenvalue, the channels with the highest amplitude within the spatial eigenvectors. In this way one discards the channels which contain the smallest amount of information for the data set. If one channel is already neglected by another eigenvector the channel with the second great amplitude is discarded. The selected channels can be very different from the first method.

An improved version of this strategy is to redo the SVD after each discarded channel with the reduced data set with a lower dimension p. This results only in a slightly different set of remaining channels.

2.3 Linear Regression Analysis for Prediction, Step 3

With the channels, selected according to the method presented in the previous section, we now describe the third step in the online determination of the total radiated power, the determination of the weighting factors for the summation over the selected channels (see equation (1)).

The regression analysis searches for a function $\hat{f}(\vec{x}(i))$ which approximates a functional relation between the multidimensional declaring quantity $\vec{x}(i)$ and a dependent quantity $y(i)$ for all available pairs of quantities i.

$$y(i) = \hat{f}(\vec{x}(i)) + \epsilon(i). \tag{10}$$

In our case the $\vec{x}(i)$ are the measurements from the bolometric camera system and $y(i)$ are the corresponding offline calculated radiated power. For each time point t_i from the selected existing discharges one gets one set of these quantities. The function is determined by the assumption of a regression model, in our case by a simple linear regression model without a constant term

$$y(i) = \hat{f}(\vec{x}(i)) + \epsilon(i) = \sum_{j=1}^{p} c_j x_j(i) + \epsilon(i). \tag{11}$$

The coefficients c_j are determined by a minimization of the error between the model and the correct inversion for all the considered times t_i

$$\sum_{i=0}^{N}(\epsilon(i))^2 \stackrel{!}{=} min, \qquad \text{with:} \quad \epsilon(i) = y(i) - \sum_{j=1}^{p} c_j x_j(i) \tag{12}$$

3 Practical Results for Discharges

After the general description of the methods in this work, we will now describe the realization and the results from this method.

3.1 Data Set for Offline Analysis (Step 1)

The first step which has to be done is the selection of a set of discharges for selecting the channels and calculating the regression coefficients. The following discharges were used for this analysis:

- NI heated discharges with H gas (positive and negative main field, various plasma currents) : #4510, #4511, #4513, #4514, #4516
- NI heated discharges with D gas and D_2 and Ne puffing (positive and negative main field, various plasma currents) : #4833, #4834, #4845, #4846, #4848, #4849, #4857, #4858*, #4862*, #4863*, #4878, #4879, #4894*, #5028, #5567*, #5577*, #5657*, #5659*, #5685
- Standard density limit discharges (I_p = 0.6 MA, B_t = -2.0 T): #2975, #2997, #3062, #3396, #3384, #2908

Discharges marked with * were done to reach the CDH-mode.

Typical discharges with impurity radiation from the plasma edge were investigated. For this reason the main part of the analyzed discharges were H-mode plasmas with neutral beam injection. For a more general description of the total radiated power also some ohmically heated density limit discharges were included in the analysis. In these standard discharges the condition of the experiment is documented by the maximum achievable density by continuously raising the density until a density limit disruption occurs.

3.2 SVD of the selected discharges and weighting factors (Step 2, Step 3)

The second and third step, the selection of the the needed channels and the determination of the regression coefficients is presented in this section. The comparison with the offline calculated results is shown separately in the following section.

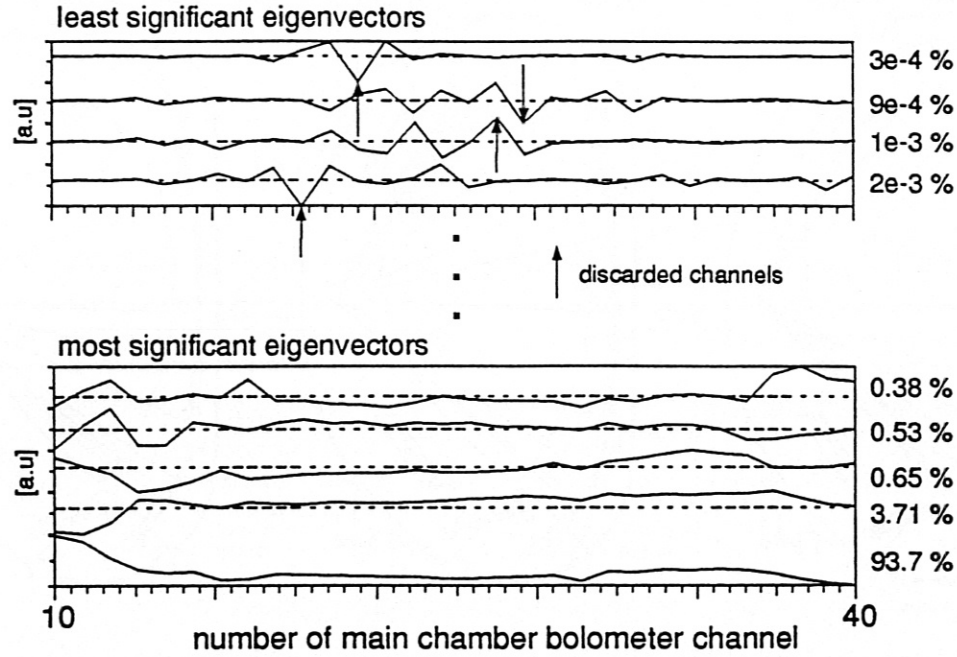

Figure 2: spatial eigenvectors for the complete set of analyzed discharges with data only from the main chamber. On the right side the relative variance of the corresponding eigenvectors is shown

Figure 2 shows the spatial eigenvectors of a SVD analysis of the complete set of discharges presented in section 3.1. The degree of information (see eq. (9)) is also shown on the right side of the picture for the most and the less significant eigenvectors.

In the very first analysis of all bolometric channels, including the 10 channels which measure the emission of the X-point and the target plates, 10 lines of sight were selected. In this case the channels were selected by examining only the most significant eigenvectors with the highest eigenvalues. From these eigenvectors the channels with the highest amplitudes were chosen for the regression analysis. The results with the according weighting factors are shown in table 1 and the first part of figure 3.

As the X-point and the divertor region are areas of cold plasma with high density, the assumption of constant emissivity on flux surfaces is no longer valid for the X-point and the flux surfaces outside the separatrix. As the X-point is a cold plasma with high density it is a strong source of radiation. So the channels looking trough the X-point and on the target plates have to be neglected before the SVD. This is done with the help of an equilibrium analysis and can vary between different discharges and also during each discharge itself. As for the online determination the selected channels can not be modified any more, we restricted the analysis to channels whose line of sight lie surely above any ever reached position of the X-point. Due to long term experience [3] we discharded channels 1-9 of the horizontal bolometer camera in the analysis. From the remaining 30 lines of sight now the SVD was done. For this analysis two different

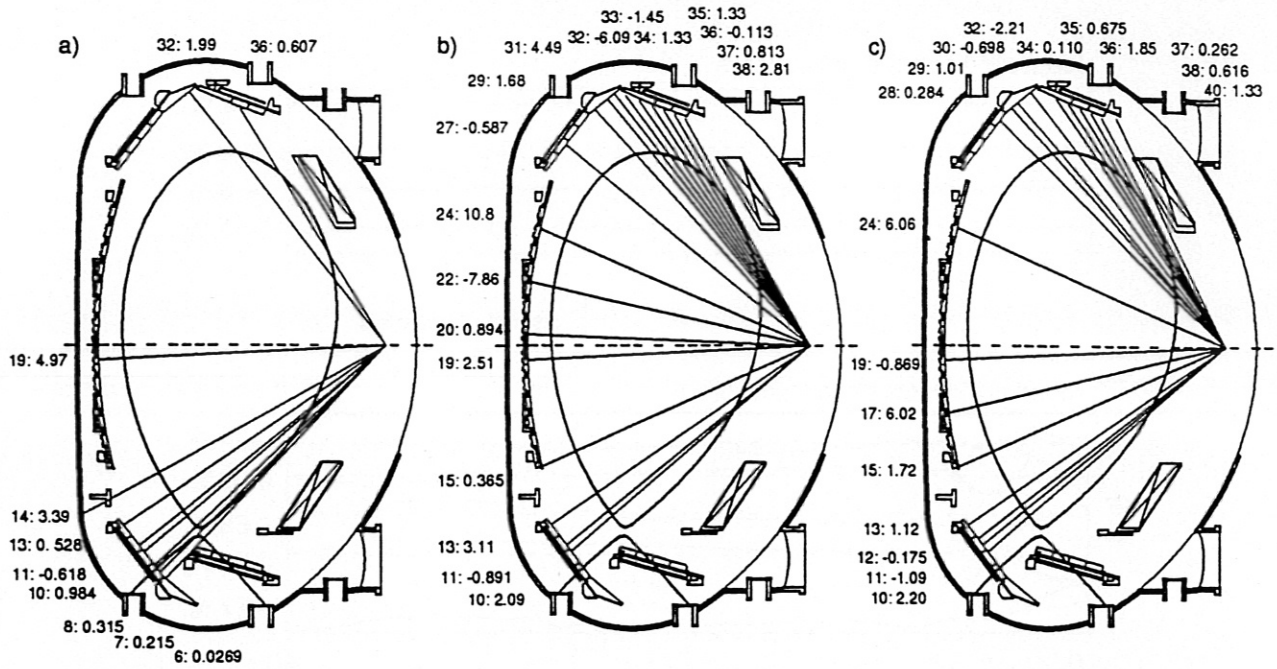

Figure 3: Selected channels for the regression analysis: a) 10 channels from the main chamber and the divertor region by selecting channels from the most significant eigenvectors, c) 18 channels from the main chamber by selecting channels from the most significant eigenvectors, and c) 18 channels from the main chamber by discarding channels from the less significant eigenvectors. The numbers next to the lines of sight show the channel number and the calculated weighting factor in m^2.

selection schemes were used. In addition to the selection of the channels with the greatest amplitude within the most significant eigenvectors the channels were chosen by neglecting the channels with the highest amplitude in the less significant spatial eigenvectors. This was done recursively, e.g. after neglecting one channel a new SVD analysis with the remaining channels was done. From the new eigenvectors the next channel was discarded and so on. In both cases not only 10 channels, but the maximum available number of 18 for were used. The results of these two runs with the according weighting factors are shown in table 2 and 3 and in the second and third part of figure 3 respectively.

3.3 Comparison between different channel selection schemes (Step 4)

After presenting a first very rude channel selection (selection of 10 channels by the most significant eigenvectors from all lines of sight) and more sophisticated methods (discarding the lines of sight in the divertor region, recursively discarding of channels by the less significant eigenvectors), now the results for the prediction of the total radiated power will be discussed.

selected channel	regression coefficient
6	0.0268666 m^2
7	0.214721 m^2
8	0.315309 m^2
10	0.984371 m^2
11	-0.617735 m^2
13	0.527544 m^2
14	3.39385 m^2
19	4.96983 m^2
32	1.98698 m^2
36	0.606678 m^2

Table 1: 10 selected channels and corresponding regression coefficients from the main chamber and the divertor region by selecting channels from the most significant eigenvectors

selected channel	regression coefficient
10	2.08726 m^2
11	-0.890637 m^2
13	3.09516 m^2
15	0.36494 m^2
19	2.50812 m^2
20	0.893842 m^2
22	-7.86491 m^2
24	10.8175 m^2
27	-0.586927 m^2
29	1.67705 m^2
31	4.4893 m^2
32	-6.08651 m^2
33	-1.44948 m^2
34	1.33246 m^2
35	1.33292 m^2
36	-0.113323 m^2
37	0.813442 m^2
38	2.80532 m^2

Table 2: 18 selected channels and corresponding regression coefficients from the main chamber without the divertor region by selecting channels from the most significant eigenvectors

selected channel	regression coefficient
10	2.20286 m^2
11	-1.09006 m^2
12	-0.174691 m^2
13	1.12282 m^2
15	1.72011 m^2
17	6.02357 m^2
19	-0.869487 m^2
24	6.05533 m^2
28	0.283516 m^2
29	1.00638 m^2
30	-0.697868 m^2
32	-2.20556 m^2
34	0.109556 m^2
35	0.674694 m^2
36	1.85254 m^2
37	0.26249 m^2
38	0.616458 m^2
40	1.32719 m^2

Table 3: 18 selected channels and corresponding regression coefficients from the main chamber without the divertor region by neglecting channels from the less significant eigenvectors

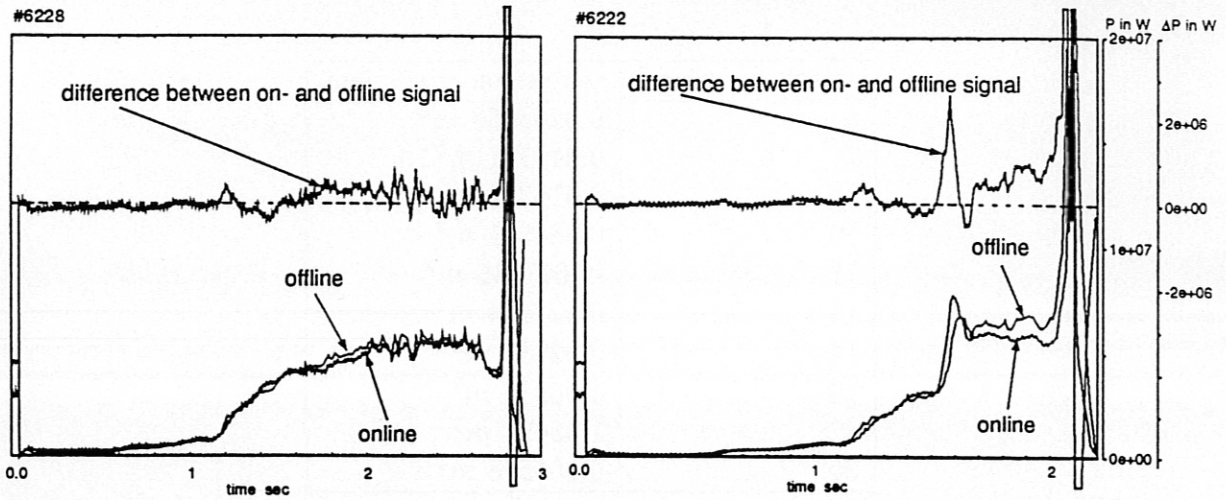

Figure 4: Comparison between online and offline calculated radiated power for the discharges #6228 and #6222. 10 lines of sight were selected from main chamber and divertor region from the most significant eigenvectors

Figure 4 shows the online and offline calculated radiated power for the two test discharges #6228 and #6222. These two discharges are CDH discharges with gas puffing of Nitrogen and Argon respectively with 1 MA plasma current and 2.5 T toroidal field. In the lower part of this and the following figures the time traces of the online and offline calculated amount of the radiated power is shown with the same scale for the radiated power in W. The upper part shows the absolute difference between these two quantities, which has to be minimized. For the discharge #6228 the results fit quite well, whereas for #6222 the agreement in the CDH-mode is bad. For this reason it was necessary to develop ways to improve the channel selection and/or the calculation of the weighting factors.

One had to realize that a greater amount of channels was necessary to improve the prediction and a new selection scheme had to be used for these lines of sight. In the first step presented here the lines of sight through the divertor region were discarded and 18 lines of sight were used. Looking at figure 5 one can see the improvement by these modifications.

A further improvement could be achieved by applying the new selection scheme where the channels with the greatest amplitudes in the less significant eigenvectors were discarded. Comparing figure 5 and 6 one can see that during the discharge the error is again reduced for the second selection scheme. Best results could be achieved for recursively neglecting channels, e.g. redoing the SVD after each discarded channel. For the first case with selecting the channels from the most significant eigenvectors one gets a mean absolute error $\langle \Delta P \rangle = 54kJ$ and a mean relative error $\langle \frac{\Delta P}{P_{offline}} \rangle = 0.066$. These errors are reduced for the second case with neglecting channels from the least significant eigenvectors. One gets a mean absolute error $\langle \Delta P \rangle = 43kJ$ and a mean

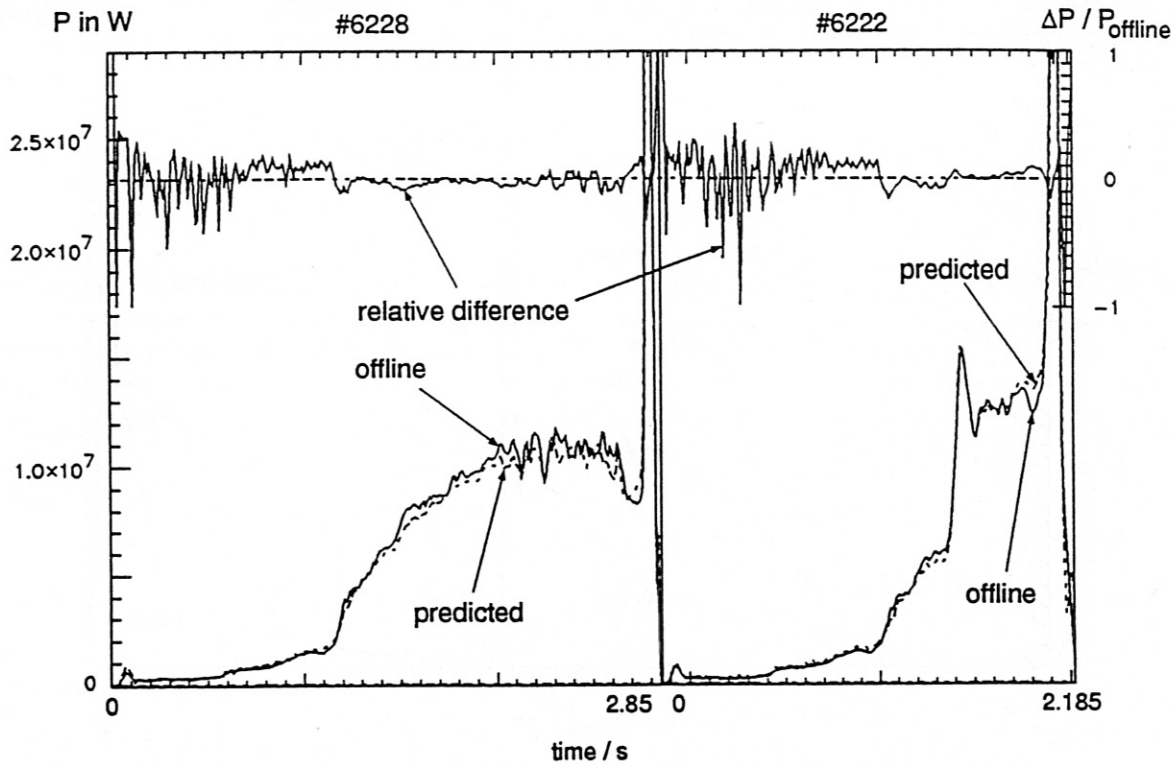

Figure 5: Comparison between online and offline calculated radiated power for the discharges #6228 and #6222. 18 lines of sight from main chamber were selected from the most significant eigenvectors. The solid line shows the offline reconstruction, the dashed line the predicted online reconstruction. The right axis shows $\Delta P/P_{offline}$ which represents the relative error.

relative error $\langle \frac{\Delta P}{P_{offline}} \rangle = 0.011$. For times when there is very low or none radiation calculated from the offline method, the relative error diverges as one has to divide through very small numbers or even zero.

3.4 Completely Detached H-Mode

A reduction of the energy flux density to the target plates is necessary for a future fusion reactor. This goal could be achieved on ASDEX Upgrade by raising the edge plasma density by gas puffing and the controlled puffing of light impurities (neon,argon) to the edge. The strong gas puffing is feedback controlled to achieve a constant neutral particle density in the divertor chamber, whereas the rate of impurity puffing is feedback controlled by the total radiated power from the main chamber.

Considering the quantity $P_{sep} = P_{heat} - P_{rad}^{bulk}$, which describes the heating power minus the radiated power from the bulk plasma without the radiation from the scrape off layer (SOL), the behavior of the ELMs in the H-mode show a similar behavior as obtained by a variation of the heating power alone without a radiating boundary [2].

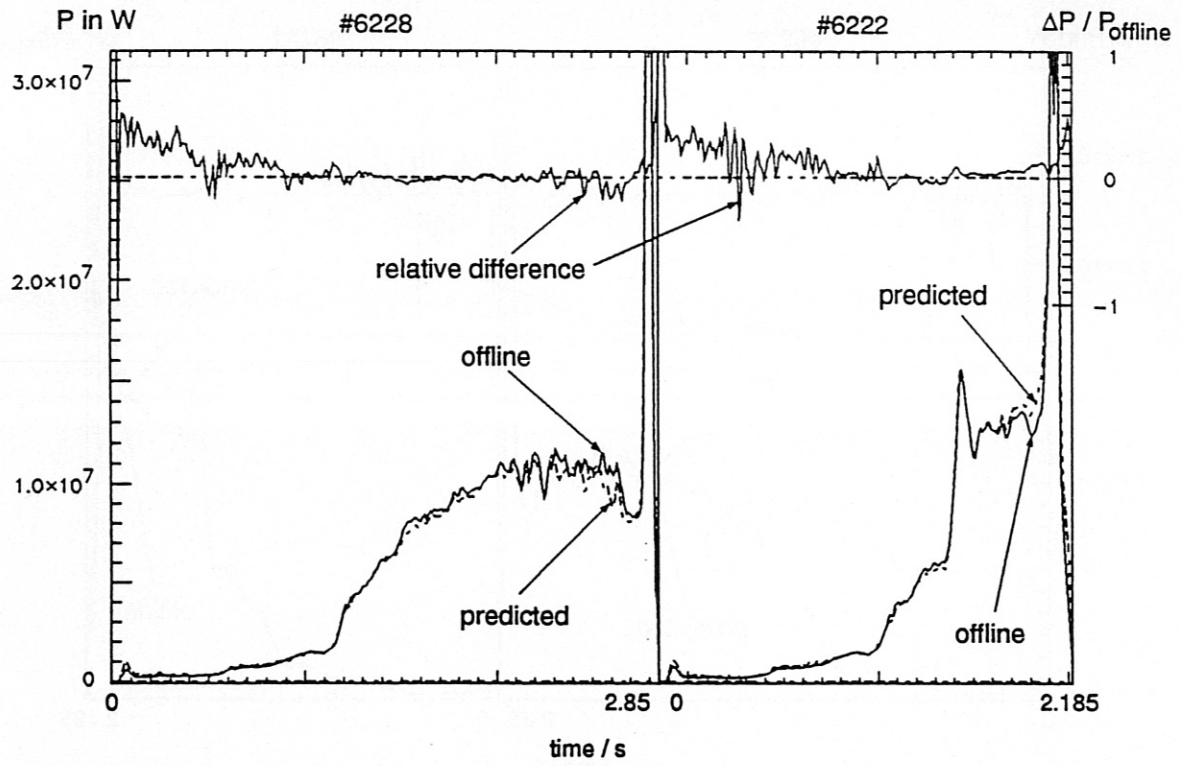

Figure 6: Comparison between online and offline calculated radiated power for the discharges #6228 and #6222. 18 lines of sight from main chamber were selected by neglecting channels from the less significant eigenvectors. The solid line shows the offline reconstruction, the dashed line the predicted online reconstruction. The right axis shows $\Delta P/P_{offline}$ which represents the relative error.

When P_{sep} is reduced remaining above the threshold for the H to L transition P_{thr}^{H-L} the type I ELMs change to type III ELMs [7] without going back to L-mode. The type III have a higher repetition frequency and a lower power deposition per ELM on the target plates and reduce in this way the power flux to the divertor. For radiated power fractions of 90% detachment from from the divertor plates occurs. This takes place when $P_{rad}^{SOL} + P_{rad}^{divertor} = P_{sep}$ is satisfied. As the discharges remains in the H-mode and has still a high energy confinement time τ_E these type of discharges are interesting candidates for a future fusion device.

With the online determination of the total radiated power presented in this work it is possible to calculate this quantity in a much better way than it was possible before with only ten channels and the old selection scheme by selecting the signals from the most significant eigenvectors.

4 Conclusion

The online determination of the total radiated power from the main plasma chamber was needed to improve the plasma feedback control on ASDEX Upgrade. This new control feature is used to control the amount of impurity puffing in order to radiate the power transported over the separatrix in the SOL before it reaches the divertor plates.

For this purpose a new selection scheme of relevant lines of sight from a 40 channel bolometric camera system was used. From the selected channels a regression analysis between this subset and a offline calculated number of the radiated power gave weighting factors for a analogue summation over the relevant channels to calculate the desired quantity.

With a strong gas puffing, which is feedback controlled with the neutral particle density in the divertor chamber, one could reach the so called completely detached H-mode (CDH-mode). Almost all the heating power is radiated by e.g. Neon in the scrape off layer of the main chamber before reaching the divertor plates [1, 2]. This could be a promising regime for future devices, such as ITER .

References

[1] O. Gruber, A. Kallenbach, M. Kaufmann, K. Lackner, V. Mertens, J. Neuhauser, F. Ryter, H. Zohm, and et al., Observation of Continuos Divertor Detachment in *H*-Mode Discharges in ASDEX Upgrade, Phys. Rev. Lett. **74**(21), 4217 – 4220 (May 1995).

[2] A. Kallenbach, R. Dux, V. Mertens, O. Gruber, G. Haas, and et al., H-mode discharges with feedback-controlled radiative boundary in the ASDEX Upgrade tokamak, Nucl. Fusion **35**(10), 1231 – 1246 (1995).

[3] J. Fuchs, private communication.

[4] M. Maraschek, Statistische Datenanalyse im Hinblick auf Früherkennung von Disruptionen am Tokamak ASDEX Upgrade, Diplomarbeit, Technische Universität München, IPP Report 1/279 (1994).

[5] F. Murtagh and A. Heck, *Multivariate Data Analysis*, Astrophysics and Space Science Library, 1987.

[6] K. V. Mardia, J. T. Kent, and J. M. Bibby, *Multivariate Analysis*, Propability and Mathematical Statistics, Academic Press, 1979.

[7] H. Zohm, Edge Localized Mode, Plasma Phys. Controlled Fusion **38**(2) (1996).